Case Studies in Thermal Engineering 41 (2023) 102609

Contents lists available at ScienceDirect

Case Studies in Thermal Engineering

journal homepage: www.elsevier.com/locate/csite

Evaluating the time lag and decrement factor of mortar and concrete containing OPBC as an agricultural by-product lightweight aggregate

Iman Asadi [a,*], Mohammad Hashemi [b,**], Behrang Sajadi [c], Norhayati Binti Mahyuddin [d,e], Mohammad Hajmohammadian Baghban [f], Masoud Esfandiari [g], Mehdi Maghfouri [h], Kezhen Yan [b]

[a] Department of Structural Engineering, Norwegian University of Science and Technology, NO 7491, Trondheim, Norway
[b] College of Civil Engineering, Hunan University, Changsha, 410082, Hunan Province, China
[c] School of Mechanical Engineering, College of Engineering, University of Tehran, Iran
[d] Department of Building Surveying, Faculty of Built Environment, University of Malaya, 50603, Kuala Lumpur, Malaysia
[e] Center for Building, Construction & Tropical Architecture (BuCTA), Faculty of Built Environment, University of Malaya, 50603, Kuala Lumpur, Malaysia
[f] Department of Manufacturing and Civil Engineering, Norwegian University of Science and Technology, Gjøvik, Norway
[g] Department of Structural, Geotechnical and Building Engineering (DISEG), Politecnico di Torino, 10100, Torino, Italy
[h] Hume Concrete Sdn Bhd, Wisma Hume, Petaling Jaya 46100, Malaysia

ARTICLE INFO

Keywords:
Time lag
Decrement factor
OPBC
Energy efficiency
Sustainable walls systems

ABSTRACT

Replace the normal weight aggregate with wastes or by-products materials is an appropriate method for producing a sustainable cement-based material. The replacement helps to have an energy-efficient component that reduces environmental impact. Time lag and decrement factors are vital wall system variables to evaluate thermal energy consumption in buildings. Thus, this study investigates the thermophysical properties of an innovative sustainable mortar and concrete containing oil palm boiler clinker (OPBC) as fine and coarse aggregate through an experimental approach. Then, time lag and decrement factor in different wall systems are calculated based on EN ISO 13786 through Python 3.7 (NumPy and math modules) and optimized using the response surface methodology (RSM). The results indicated mortar with OPBC has a slightly reduced decrement factor and increased time lag compared to a typical mortar. More significantly, the decrement factor of OPBC concrete was reduced by 34%, and its time lag increased up to 58% compared to conventional concrete.

* Corresponding author.
** Corresponding author.
E-mail addresses: asadi8564@gmail.com, iman.asadi@ntnu.no (I. Asadi), hashemimohammad23@yahoo.com (M. Hashemi).

https://doi.org/10.1016/j.csite.2022.102609
Received 5 July 2022; Received in revised form 2 October 2022; Accepted 28 November 2022
Available online 2 December 2022

Nomenclature

A	Amplitude
C	Specific heat capacity (J/g.°C)
d	The thickness of layer (m)
f	Decrement factor
h	Convective and radiative heat transfer coefficient (W/m^2 °C)
j	Imaginary axis of a complex number $j^2 = -1$
k	Thermal conductivity (W/m.°C)
q	Heat flux (W/m^2)
Q	Heat flow (W)
R	Thermal resistance (°C/W)
t	Time (sec)
T	Temperature (°C)
U	Thermal transmittance (W/m^2 °C)
V	The volume of samples (m^3)
Z	Heat transfer matrix
ρ	Density (kg/m^3)
φ	Time lag
δ	periodic penetration of heatwave (m)
μ	The ratio of layer thickness to the penetration thickness
τ	Period

Acronyms

ANOVA	Analysis of Variance
NC	Normal concrete
NM	Normal mortar
OPBC	Oil palm boiler clinker
OPBCC	Oil palm boiler clinker mortar
OPBCM	Oil palm boiler clinker mortar
OPC	Ordinary Portland Cement
OPS	Oil palm shell
PCA	Portland Cement Association
PRESS	predicted residual error sum of square
RSM	Response Surface Methodology
SSD	Saturated-surface-dry

Subscripts and superscripts

a	Ambient
c	Cooling
in	Inside
max	Maximum
min	Minimum
out	Outside
p	constant pressure
sa	Soil-air
w	Wall

1. Introduction

The thermal properties of mortar and concrete are influenced by the thermal properties of their ingredients and the volume ratio of the raw materials, such as fine and coarse aggregates, water, and cementitious materials [1]. Aggregates account for 60–75% of the total volume of concrete; therefore, the thermal properties are mainly influenced by aggregate [2]. Also, the aggregate volume fraction significantly impacts the thermal conductivity (k), specific heat capacity (C_p), and thermal diffusivity of cement mortar and concrete [3–5].

Prior studies evaluated the physical and mechanical properties of concrete containing oil palm shell (OPS) and oil palm boiler clinker (OPBC) as aggregate [6–12]. However, no study assesses the thermophysical properties of concrete containing OPBC as fine and coarse aggregate. Lower k and higher C_p of OPBC compared to the normal aggregates [13] indicates there is a great potential to reduce the thermal energy consumption of buildings by using mortar and concrete containing OPBC aggregates. Therefore, despite its

importance, the assessment of the dynamic thermal properties related to OPBC mortar and concrete in a wall system has not been considered in the literature.

It is vital to determine a wall system's dynamic thermal properties and heat transfer using transient conditions to achieve robust and reliable thermal comfort and energy efficiency prediction in buildings [14]. In an actual situation, the variation of outdoor temperature resulting the wall absorbing the heat when $T_{out} > T_w$ and releasing it back to the surroundings when $T_o < T_w$. The thermal inertia of the wall depends on dynamic thermal properties [15]. Time lag (φ) and decrement factor (f) are the essential dynamic parameters to evaluate the heat storage capacity of a wall system. A heatwave has a specific amplitude and a specific wavelength. As a thermal mass, the wall system reduces the heatwave amplitude [16]. The time lag represents the time variance between the heatwave peaks occurring outdoors and indoors. Also, the decrement factor describes the amplitude ratio of the heatwave before and after passing through the wall [17].

The prior literature indicated a gap in knowledge where dynamic thermal properties should be studied for innovative materials in the construction industry. Primarily, thermal conductivity has been evaluated as an indicator of a material's thermal behavior; however, heat capacity identification is also vital for these materials. Thus, this study first measures the thermophysical properties of OPBC concrete, which have not yet been evaluated in the literature. It should be noted that although ref [13] has measured the thermal properties of OPBC mortar, this study evaluates and compares the dynamic thermal properties of cement mortar and concrete -time lag and decrement factor-with and without OPBC. Finally, the impact of the OPBC wall system on the indoor air temperature is investigated, which has not been considered in previous studies.

2. Experimental program

Five different mortar and concrete mixtures were prepared to evaluate the effect of OPBC on their physical, mechanical, and thermal properties. Table 1 presents the mix design of cement mortar and concrete without any OPBC (regular mixture of mortar and concrete), cement mortar containing OPBC instead of sand (OPBC mortar), concrete containing OPBC as coarse aggregate (OPBC concrete 1), and concrete containing OPBC as both fine and coarse aggregate (OPBC concrete 2).[1]

The compressive strength test of mortar and concrete were respectively carried out according to ASTM C109 [18] and ASTM C39 [19] at the curing age of 28 days. The KD2-Pro was employed to measure the samples' thermal conductivity (the specimens with a length of 100 mm and height of 200 mm) under both oven-dried (Dried in the oven at 105 °C for 24 h) and SSD conditions. The heat capacity of raw materials was measured by DSC (METTLER TOLEDO 820C) from 30 to 50 °C in the air atmosphere. Then the mixture law was applied to calculate the heat capacity of the samples [13].

3. Time lag (φ) and decrement factor (f)

Determination of a wall system's time lag and decrement factor is necessary when the boundary conditions are periodic. The minimum and maximum time lag are identical when the boundary condition is Sine–type periodic [20]. The maximum and minimum time lag and decrement factor can be defined as follows [15]:

$$\varphi_{max} = t_{in,max} - t_{out,max} \tag{1}$$

$$\varphi_{min} = t_{in,min} - t_{out,min} \tag{2}$$

$$f = \frac{A_{in}}{A_{out}} = \frac{T_{in,max} - T_{in,min}}{T_{out,max} - T_{out,min}} \tag{3}$$

EN ISO 13786 [21] suggested a matrix formulation to calculate the time lag and decrement factor. These equations are adapted from the analytic solution of the heat transfer equations. The thermal resistance of a single layer is:

$$R_t = R_{si} + \frac{l}{k} + R_{so} \tag{4}$$

and the thermal transmittance (U) is:

$$U = \frac{1}{R_t} \tag{5}$$

Thus, the heat transfer correlation matrix between outside and inside for one layer of the wall is

$$Z = \begin{pmatrix} T_2 \\ q_2 \end{pmatrix} = \begin{pmatrix} Z_{11} & Z_{12} \\ Z_{21} & Z_{22} \end{pmatrix} \begin{pmatrix} T_1 \\ q_1 \end{pmatrix} \tag{6}$$

The matrix elements can be calculated as follow:

[1] reference binder: Ordinary Portland Cement (OPC) with a specific gravity of 3.14 and a specific surface area of 3510 cm^2/g.fine aggregate: mining sand with water absorption of 1.5%, fineness modulus of 2.9, and saturated-surface-dry (SSD) specific gravity of 2.55. Also, OPBC with SSD specific gravity, fineness modulus, and water absorption of 2.11, 2.71, and 5 ± 1%. Coarse aggregate: normal crushed coarse aggregate with the maximum nominal size, 24 h water absorption, and SSD specific gravity of 19 mm, 0.67%, and 2.62. Also, OPBC with SSD specific gravity, fineness modulus, and water absorption of 1.82, 6.75, and 3 ± 1%.

Table 1
The mixed proportions details.

	Mix ID	Cement (kg/m^3)	Normal Fine Aggregate (kg/m^3)	Normal Coarse Aggregate (kg/m^3)	OPBC Fine Aggregate (kg/m^3)	OPBC Coarse Aggregate (kg/m^3)	W/C
Concrete	Normal Concrete (NC)	400.0	840.0	950.0	0	0	0.53
	OPBC Concrete 1 (OPBCC1)	468.4	773.4	0	0	555.5	0.32
	OPBC Concrete 2 (OPBC2)	498.1	0	0	590.8	648.7	0.32
Mortar	Normal Mortar (NM)	488.8	1466.6	0	0	0	0.5
	OPBC Mortar (OPBCM)	604.8	0	0	982.8	0	0.5

$$Z_{11} = Z_{22} = \cosh(\mu)\cos(\mu) + j\sinh(\mu)\sin(\mu) \tag{7}$$

$$Z_{12} = -\frac{\delta}{2k}\{\sinh(\mu)\cos(\mu) + \cosh(\mu)\sin(\mu) + j[\cosh(\mu)\sin(\mu) - \sinh(\mu)\cos(\mu)]\} \tag{8}$$

$$Z_{21} = -\frac{\delta}{k}\{\sinh(\mu)\cos(\mu) - \cosh(\mu)\sin(\mu) + j[\cosh(\mu)\sin(\mu) + \sinh(\mu)\cos(\mu)]\} \tag{9}$$

Where ᴍ is defined as the ratio of the thickness to the penetration depth:

$$\mu = \frac{d}{\delta} \tag{10}$$

The periodic penetration is calculated with the following equation:

$$\delta = \sqrt{\frac{k.\tau}{\pi.\rho.C}} \tag{11}$$

Finally, the heat transfer matrix from the outside to the inside is:

$$Z_{out-in} = Z_{s2}\, Z\, Z_{s1} \tag{12}$$

Where, Z_{s2} , Z_{s1} are the heat transfer matrixes of inside and outside based on convection and radiation values. The standard value for R_s is described in ISO6946 [22] as

$$Z_s = \begin{pmatrix} 1 & -R_s \\ 0 & 1 \end{pmatrix} \tag{13}$$

Thus, the periodic thermal transmittance is:

$$Y_{12} = -\frac{1}{Z_{12}} \tag{14}$$

The time lag is:

$$\varphi = \frac{\tau}{2\pi}\arg\, Y_{12} \tag{15}$$

And the decrement factor is:

$$f = \frac{|Y_{12}|}{U} \tag{16}$$

It should be noted that the matrix Z in equation (12) for a multilayer wall is defined as:

$$Z = \begin{pmatrix} Z_{11} & Z_{12} \\ Z_{21} & Z_{22} \end{pmatrix} = Z_n Z_{n-1} Z_3 Z_2 Z_1 \tag{17}$$

Table 2
The wall layers.

Type of concrete	Layers from inside to the outside			
NC	NM–NC–NM (I)	NM–NC–OPBCM (II)	OPBCM–NC–NM (III)	OPBCM–NC–OPBCM (IV)
OPBCC1	NM-OPBC1-NM (V)	NM-OPBC1-OPBCM (VI)	OPBCM-OPBC1-NM (VII)	OPBCM-OPBC1-OPBCM (VIII)
OPBCC2	NM-OPBC2-NM (IX)	NM-OPBC2-OPBCM (X)	OPBCM-OPBC2-NM (XI)	OPBCM-OPBC2-OPBCM (XII)

Since time lag and decrement factor values are not influenced by climate, the following equation can be hired to determine the soil-air temperature:

$$T_{sa}(t) = \frac{T_{max} - T_{min}}{2} \sin\left(\frac{2\pi t}{P} - \frac{\pi}{2}\right) + \frac{T_{max} + T_{min}}{2} \quad (18)$$

4. Climate and wall system

Kuala Lumpur, the capital of Malaysia, has a tropical rainforest climate where the temperature is usually high throughout the year, and there is high humidity [23]. Identifying the hottest day of the year is vital to design building envelopes and HVAC systems. Then, this study selected the minimum and maximum temperatures of the hottest day for heat transfer analysis. To analyze the heat transfer through the external wall of buildings, 12 wall systems were considered. Table 2 illustrates the wall topology and materials used for each wall layer. The thickness of the external wall is varied based on the design need. Also, cement mortar may be applied to plaster an outer wall's interior and exterior surface in various thicknesses. To cover a variety of possibilities; therefore, the dynamic thermal properties of concrete and cement mortar are calculated in the range of 100–200 mm and 5–25 mm, respectively. In this study, Design expert software was hired to design the wall thickness with different layers. The thickness of interior mortar, concrete, and exterior mortar was considered the three numerical factors. Time lag and decrement factor were defined as the desired responses.

5. Results and discussions

5.1. Experimental measurements

The results showed that the compressive strength of mortar and concrete decreased significantly using OPBC as the aggregate. The replacement of normal sand with OPBC (fine aggregate) reduced the compressive strength of mortar by around 46%. Also, the compressive strength of concrete decreased by approximately 16% and 29% when the OPBC was used as the only coarse aggregate and coarse and fine aggregate, respectively. The findings of this study agree with available literature that reported the compressive strength of cement mortar and concrete in the ranges of 20.3–61.67 MPa [6,24–26].

Regarding the density of samples, OPBCM, OPBCC1, and OPBCC2 are considered lightweight mortar and concrete with densities of 1890 kg/m^{3,} 1950 kg/m^3, and 1900 kg/m^3, respectively. The achieved results are in agreement with the available literature, which demonstrated the density of OPBC mortar (OPBC as fine aggregate) in the ranges of 1520–1940 kg/m^3 [27–29] and OPBC concrete (OPBC as finding and/or coarse aggregate) in the ranges of 1440–2030 kg/m^3 [30,31].

In the cases of thermal conductivity and specific heat capacity, the results indicated that utilizing OPBC as aggregate in mortar and

Table 3
Thermal conductivity, specific heat capacity, and density of samples.

Mix ID	Density (kg/m^3)	Compressive strength (MPa)	Thermal conductivity (W/m.K)		Specific heat capacity (J/kg.K)	Thermal diffusivity (m^2/s)
			Oven dry	SSD		
NC	2400	48.3	2.86	3.00	1010	1.17987E-06
OPBCC1	1950	41.1	1.01	1.62	1018	5.0879E-07
OPBCC2	1900	34.6	0.77	1.27	1243	3.26036E-07
NM	2200	61.3	2.67	2.87	980	1.2384E-06
OPBCM	1890	32.7	0.74	1.02	1178	3.32372E-07

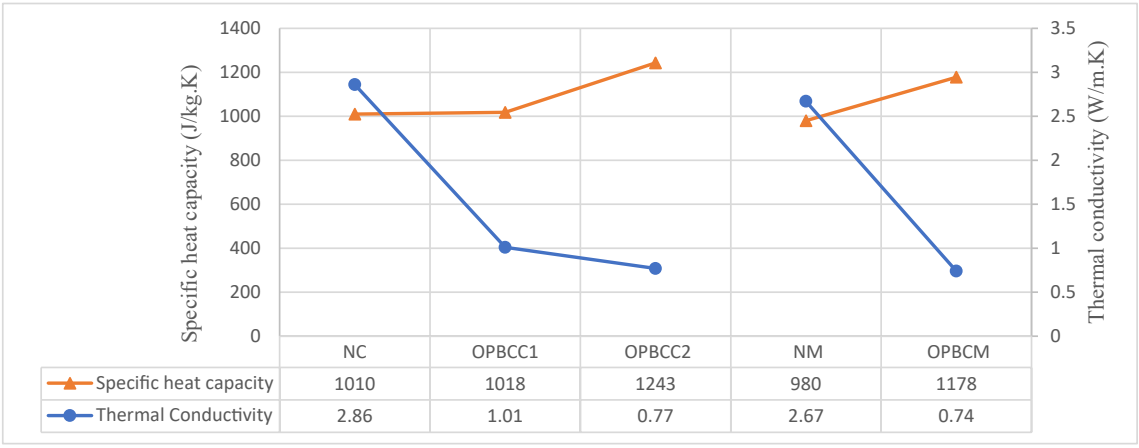

Fig. 1. Thermal conductivity vs. heat capacity.

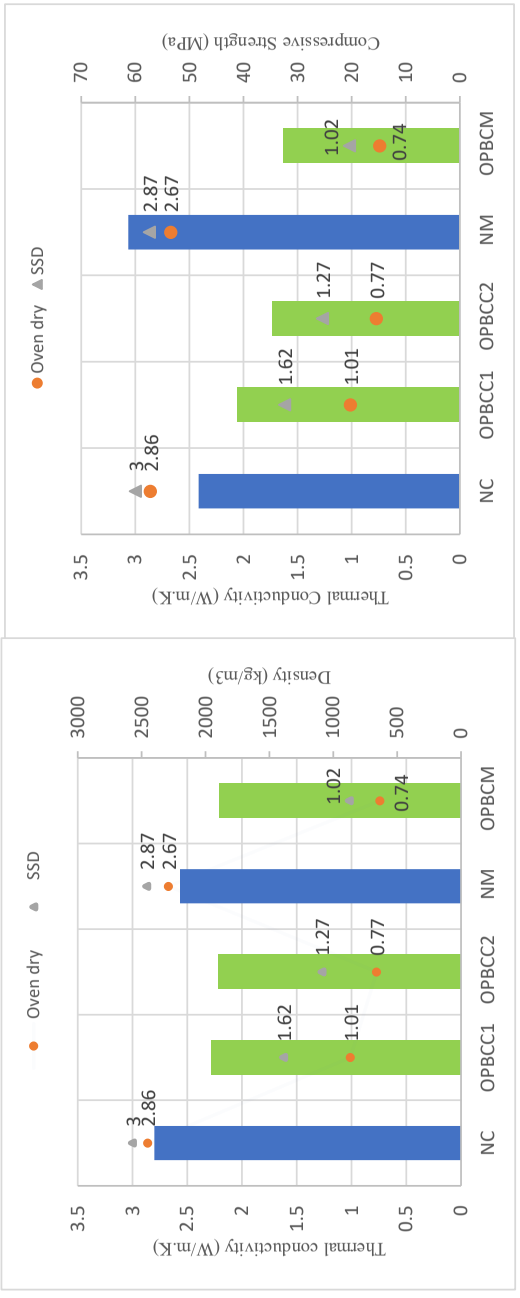

Fig. 2. Thermal conductivity vs. a: Density and b: Compressive strength.

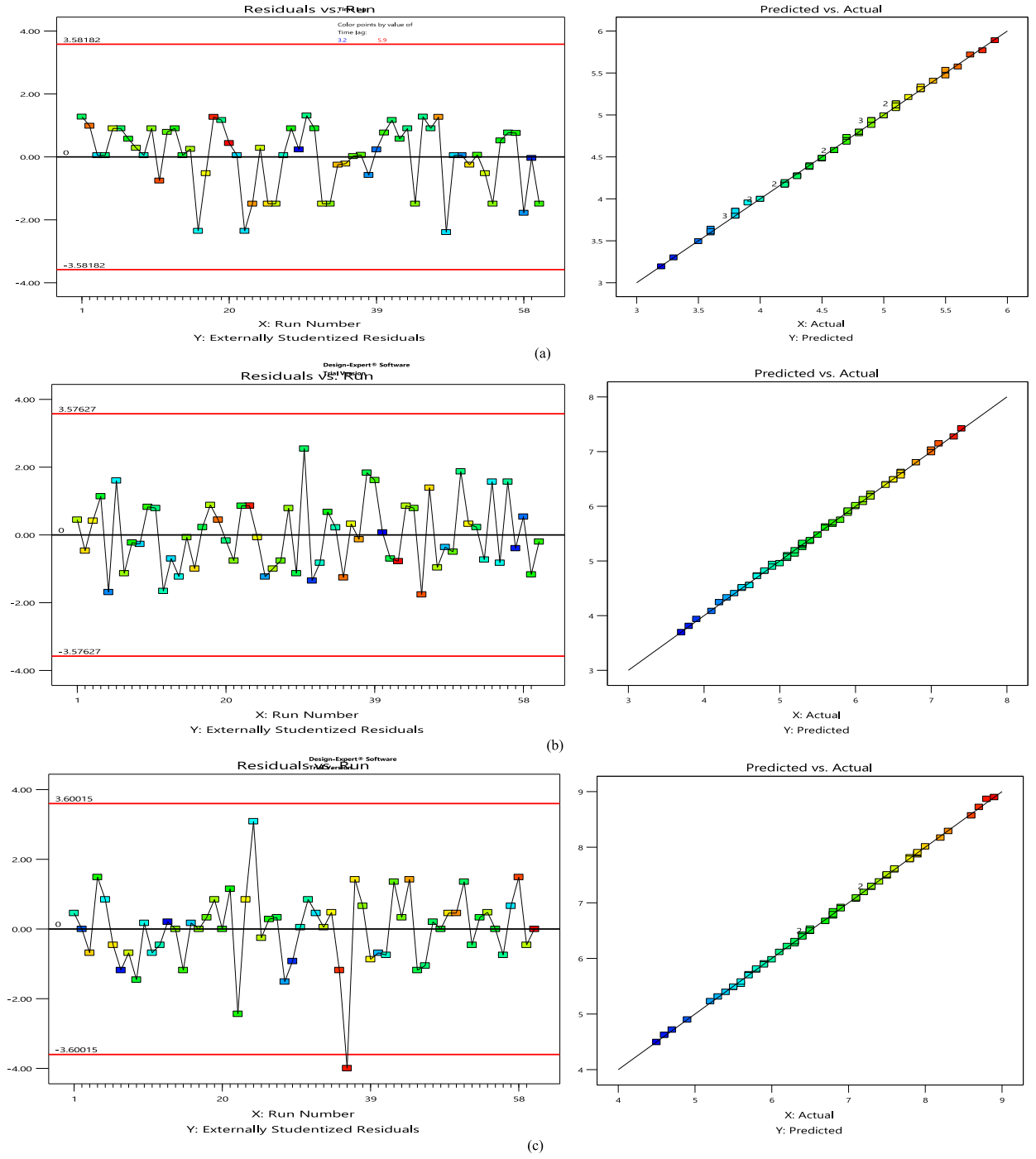

Fig. 3. Residual vs. run number and calculated vs. predicted time lag values for a: NC, b: OPBCC1, and c: OPBCC2.

concrete significantly reduces thermal conductivity and increases heat capacity (Table 3). The porous nature of OPBC can be the main reason for reducing thermal conductivity [13]. The findings are plotted in Figs. 1 and 2.

5.2. *Dynamic thermal properties of single-layer*

The dynamic thermal properties of mortar and concrete were calculated according to EN ISO 13786 in the ranges of 5–25 mm (interval of 5 mm) and 100–200 mm (interval of 20 mm), respectively. Equations (4)–(16) were coded in Python 3.7 using NumPy and math modules (Appendix A). The U-value, time lag, and decrement factor of different materials for various thicknesses are summarized in Table 4 and Table 5.

Table 4
Dynamic thermal properties of mortar in different thickness.

	5 mm		10 mm		15 mm		20 mm		25 mm	
	Φ (h)	f	Φ (h)	f	Φ (h)	f	Φ (h)	f	Φ (h)	f
NM	0.09	0.99	0.19	0.99	0.29	0.99	0.39	0.99	0.49	0.99
OPBCM	0.10	0.99	0.21	0.99	0.34	0.99	0.47	0.99	0.62	0.98

Table 5
Dynamic thermal properties of concrete in different thickness.

	100 mm		120 mm		140 mm		160 mm		180 mm		200 mm	
	Φ (h)	f	Φ (h)	f	Φ (h)	f	Φ (h)	f	Φ (h)	f	Φ (h)	f
NC	2.49	0.84	3.00	0.78	3.51	0.72	3.99	0.67	4.46	0.61	4.92	0.56
OPBCC1	2.85	0.83	3.55	0.77	4.24	0.69	4.92	0.62	5.59	0.56	6.25	0.50
OPBCC2	3.65	0.76	4.51	0.67	5.35	0.59	6.18	0.51	6.99	0.44	7.80	0.37

The results show that the time lag of NM and OPBCM is around 5 and 6 times higher, respectively, when the thickness is 25 mm compared to 5 mm. Particularly in higher thicknesses, the time lag significantly increases having OPBCM instead of NM in mortar or concrete. For instance, having 5 mm thinness, the time lag is around 11% more for OPBCM than NM. However, when the thickness is 25 mm, the time lag is higher, about 26%.

These findings indicated the time lag of all the concrete mixtures increased. OPBCC1 showed the highest increment in the time lag, with around 120% having thickness increased to 200 mm. Also, OPBCC1 and OPBCC2 can increase the time lag of a 200 mm one-layer concrete wall up to 27% and 58%, respectively. The time lag is an essential factor demonstrating the material's ability to postpone the outdoor temperature penetrating indoors through construction elements. This factor is directly related to a wall system's thermal properties and thickness.

5.3. Dynamic thermal properties of the wall system

Building envelopes with a higher time lag and a lower decrement factor are appropriate systems to reduce energy consumption and enhance indoor thermal comfort. Design expert software's response surface methodology (RSM) was employed to develop a predicting method and statistical evaluation. The variable factors include the central wall thickness and internal and external thickness. Internal and external finishing type was the nominal factor. The responses, including time lag and decrement factor of different wall typologies, are shown in Table 6. The time lag and decrement factor of multiple layers wall was computed by applying equations (4)–(17).

According to the results, concrete containing OPBC as fine and coarse aggregate is significantly resistant to heat transfer. The results indicated that OPBC concrete increased the time lag and reduced the decrement factor compared to conventional ones. For instance, the wall system's time lag increased to 8.9 h when OPBC replaced the traditional mortar and concrete. The effectiveness of OPBC mortar is considerably more when covering both sides of the wall. For instance, in a 200 mm NC wall, applying 15 mm OPBC mortar on both sides increased the time lag by around 7%. Also, the time lag increment is approximately 5.5% and 3.4% for the OPBCC1 and OPBCC2 walls, respectively. Considering all the results, the impact of OPBC mortar is more noticeable on conventional concrete walls.

5.3.1. Analysis of variance (ANOVA) for the time lag (φ)

As shown in Table 7, the models with a p-value less than 0.05 are statistically significant. Based on the findings, A, B, C, D, AD, CD, and B^2 are the essential factors for standard concrete. Concerning concrete with OPBC coarse aggregate, the significant factors are the A, B, C, D, AD, and CD. In the case of concrete having OPBC as both coarse and fine aggregate, the crucial factors are identified as A, B, C, D, AB, AD, and BD.

The results confirmed that the concrete thickness has a consequential impact on the time lag of a wall system. The R-squared adjusted and predicted R-squared for all three cases agree with each other and are close to 1. This indicates that the proposed model accurately predicted the time lag of the wall systems. Also, the predicted residual error sum of squares (PRESS) shows the difference between actual and predicted values [32]. The PRESS of NC, OPBCC1, and OPBCC2 are 0.071, 0.081, and 0.052, respectively. These values demonstrate a good agreement between actual and predicted values (Fig. 3).

Therefore, the following equations can be applied to predict the wall's time lag (φ) considering the component's thickness. It should be noted that the proposed equations just included significant factors.

➢ For NC:

- NM-NM:

$$\varnothing = \left[-0.06219 + \left(0.02^{*}d_{m,in}\right) + \left(0.028471^{*}d_{c}\right) + \left(0.02^{*}d_{m,ext}\right) - \left((1.90698E-005)^{*}d_{c}^{2}\right)\right] \quad (19)$$

- NM-OPBCM:

$$\varnothing = \left[-0.14302 + \left(0.02125^{*}d_{m,in}\right) + \left(0.028471^{*}d_{c}\right) + \left(0.03125^{*}d_{m,ext}\right) - \left((1.90698E-005)^{*}d_{c}^{2}\right)\right] \quad (20)$$

Table 6
The time lag of different wall systems.

Interior Mortar (mm)	Concrete (mm)	Exterior mortar (mm)	NC								OPBCC1								OPBCC2							
			I		II		III		IV		V		VI		VII		VIII		IX		X		XI		XII	
			φ	f	φ	f	φ	f	φ	f	φ	f	φ	f	φ	f	φ	f	φ	f	φ	f	φ	f	φ	f
25	150	15	4.6	0.59	4.7	0.58	5.1	0.51	5.2	0.50	5.6	0.57	5.7	0.55	6.0	0.51	6.2	0.5	6.8	0.47	6.9	0.45	7.2	0.42	7.3	0.41
10	175	10	4.7	0.57	4.8	0.57	4.9	0.54	5	0.53	5.9	0.53	6.0	0.52	6.1	0.51	6.2	0.5	7.3	0.42	7.4	0.41	7.5	0.40	7.5	0.39
10	175	20	4.9	0.55	5.1	0.54	5.1	0.51	5.3	0.50	6.2	0.50	6.4	0.48	6.4	0.48	6.6	0.46	7.6	0.40	7.8	0.38	7.8	0.38	7.9	0.36
20	125	20	4.0	0.66	4.2	0.65	4.4	0.59	4.6	0.58	4.8	0.64	5.0	0.63	5.2	0.59	5.3	0.58	5.8	0.55	6.0	0.53	6.1	0.51	6.3	0.49
20	175	20	5.1	0.53	5.3	0.51	5.5	0.47	5.7	0.45	6.5	0.49	6.6	0.47	6.8	0.44	7.0	0.43	7.8	0.38	8.0	0.37	8.2	0.35	8.3	0.33
15	150	15	4.4	0.62	4.5	0.6	4.7	0.56	4.8	0.55	5.4	0.58	5.5	0.57	5.6	0.55	5.8	0.53	6.5	0.48	6.7	0.45	6.8	0.45	6.9	0.44
15	150	5	4.2	0.64	4.2	0.64	4.5	0.59	4.5	0.58	5.1	0.62	5.1	0.61	5.3	0.58	5.4	0.57	6.2	0.51	6.3	0.50	6.5	0.48	6.5	0.47
15	150	25	4.6	0.59	4.8	0.58	4.9	0.54	5.1	0.52	5.7	0.59	5.9	0.53	5.9	0.52	6.1	0.5	6.8	0.46	7.1	0.44	7.1	0.43	7.3	0.41
10	125	10	3.6	0.71	3.6	0.71	3.8	0.67	3.8	0.67	4.2	0.70	4.3	0.69	4.4	0.67	4.5	0.66	5.2	0.60	5.3	0.59	5.4	0.58	5.5	0.57
15	100	15	3.2	0.76	3.3	0.75	3.5	0.71	3.6	0.70	3.7	0.75	3.8	0.74	3.9	0.72	4.1	0.71	4.5	0.68	4.6	0.67	4.7	0.64	4.9	0.63
10	125	20	3.8	0.69	3.9	0.67	4.0	0.65	4.2	0.63	4.6	0.66	4.7	0.65	4.7	0.64	4.9	0.62	5.6	0.57	5.7	0.55	5.7	0.55	5.9	0.53
20	125	10	3.8	0.68	3.8	0.68	4.2	0.62	4.3	0.61	4.5	0.67	4.6	0.67	4.8	0.63	4.9	0.62	5.5	0.58	5.6	0.57	5.8	0.54	5.9	0.53
5	150	15	4.2	0.64	4.3	0.63	4.3	0.62	4.4	0.61	5.1	0.60	5.3	0.59	5.2	0.59	5.3	0.58	6.3	0.52	6.4	0.49	6.4	0.49	6.5	0.47
20	175	10	4.9	0.55	5.0	0.54	5.3	0.49	5.4	0.48	6.2	0.51	6.2	0.50	6.5	0.47	6.6	0.46	7.5	0.40	7.6	0.40	7.9	0.37	7.9	0.36
15	200	15	5.5	0.49	5.6	0.48	5.8	0.44	5.9	0.43	7.0	0.44	7.1	0.42	7.3	0.41	7.4	0.39	8.6	0.35	8.7	0.32	8.8	0.31	8.9	0.30

Table 7
ANOVA for the time lag.

Source	NC					OPBCC1					OPBCC2				
	Sum of squares	df	Mean square	F-value	p-value	Sum of squares	df	Mean square	F-value	p-value	Sum of squares	df	Mean square	F-value	p-value
Model	*25.09*	*21*	*1.19*	*1585.21*	*<0.0001*	*49.67*	*18*	*2.76*	*2997.14*	*<0.0001*	*71.55*	*18*	*3.97*	*6737.83*	*<0.0001*
A	*1.50*	*1*	*1.50*	*1991.13*	*<0.0001*	*1.76*	*1*	*1.76*	*1906.77*	*<0.0001*	*1.66*	*1*	*1.66*	*2809.88*	*<0.0001*
B	*20.70*	*1*	*20.70*	*27469.47*	*<0.0001*	*44.56*	*1*	*44.56*	*48391.54*	*<0.0001*	*66.63*	*1*	*66.63*	*1.129E005*	*<0.0001*
C	*1.05*	*1*	*1.05*	*1394.04*	*<0.0001*	*1.96*	*1*	*1.96*	*2128.74*	*<0.0001*	*2.00*	*1*	*2.00*	*3381.97*	*<0.0001*
D	*1.60*	*3*	*0.53*	*709.43*	*<0.0001*	*1.25*	*3*	*0.42*	*451.03*	*<0.0001*	*1.12*	*3*	*0.37*	*633.12*	*<0.0001*
AB	*1.250E-003*	*1*	*1.250E-003*	*1.66*	*0.2056*	*1.250E-003*	*1*	*1.250E-003*	*1.36*	*0.2507*	*2.812E-003*	*1*	*2.812E-003*	*4.77*	*0.0348*
AC	*0.000*	*1*	*0.000*	*0.000*	*1.000*	*0.000*	*1*	*0.000*	*0.000*	*1.0000*	*3.125E-004*	*1*	*3.125E-004*	*0.53*	*0.4709*
AD	*0.16*	*1*	*0.054*	*71.04*	*<0.0001*	*0.13*	*3*	*0.042*	*45.48*	*<0.0001*	*0.098*	*3*	*0.033*	*55.36*	*<0.0001*
BC	*1.250E-003*	*1*	*1.250E-003*	*1.66*	*0.2056*	*1.250E-003*	*1*	*1.250E-003*	*1.36*	*0.2507*	*3.125E-004*	*1*	*3.125E-004*	*0.53*	*0.4709*
BD	*3.750E-003*	*3*	*1.250E-003*	*1.66*	*0.1922*	*3.125E-003*	*3*	*1.042E-003*	*1.13*	*0.3476*	*0.012*	*3*	*3.906E-003*	*6.62*	*0.0009*
CD	*0.051*	*3*	*0.017*	*22.39*	*<0.0001*	*0.024*	*3*	*7.917E-003*	*8.60*	*0.0002*	*0.035*	*3*	*0.012*	*20.04*	*<0.0001*
A^2	*3.419E-004*	*1*	*3.419E-004*	*0.45*	*0.5047*										
B^2	*4.188E-003*	*1*	*4.188E-003*	*5.56*	*0.0237*										
C^2	*3.419E-004*	*1*	*3.419E-004*	*0.45*	*0.5047*										
Residual	*0.029*	*38*	7.537E-004			*0.038*	*41*	*9.207E-004*			*0.024*	*41*	*5.899E-004*		
Std. Dev	*0.027*					*0.030*					*0.024*				
PRESS	*0.071*					*0.081*					*0.052*				
R-square	*0.9989*					*0.9992*					*0.9997*				
Adj- R-square	*0.9982*					*0.9989*					*0.9995*				
Pred- R-square	*0.9972*					*0.9984*					*0.9993*				

A: Interior thickness; B: Concrete Thickness; C: Exterior thickness; D: Type of Mortar.

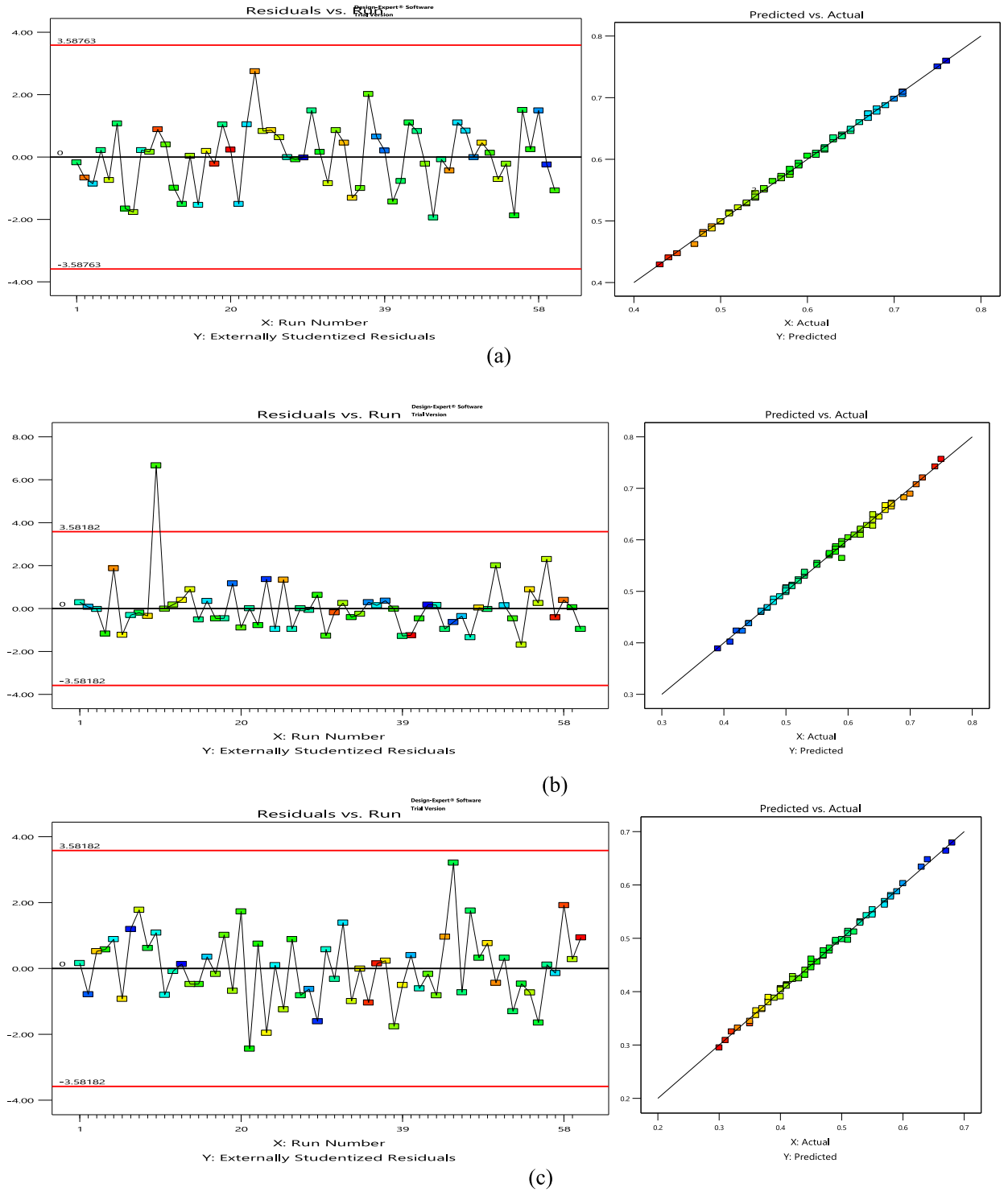

Fig. 4. Residual vs. run number and calculated vs. predicted values of decrement factor for a: NC, b: OPBCC1, and c: OPBCC2.

Table 8
ANOVA for decrement factor.

Source	NC					OPBCC1					OPBCC2				
	Sum of squares	df	Mean square	F-value	p-value	Sum of squares	df	Mean square	F-value	p-value	Sum of squares	df	Mean square	F-value	p-value
Model	*0.37*	*21*	*0.018*	*1546.32*	*< 0.0001*	*0.46*	*21*	*0.022*	*579.96*	*< 0.0001*	*0.51*	*21*	*0.024*	*829.12*	*< 0.0001*
A	*0.025*	*1*	*0.025*	*2168.37*	*< 0.0001*	*0.013*	*1*	*0.013*	*349.20*	*< 0.0001*	*0.013*	*1*	*0.013*	*434.36*	*< 0.0001*
B	*0.29*	*1*	*0.29*	*25253.91*	*< 0.0001*	*0.41*	*1*	*0.41*	*10730.8*	*< 0.0001*	*0.46*	*1*	*0.46*	*15753.15*	*< 0.0001*
C	*0.012*	*1*	*0.012*	*1057.69*	*< 0.0001*	*0.016*	*1*	*0.016*	*429.23*	*< 0.0001*	*0.013*	*1*	*0.013*	*453.88*	*< 0.0001*
D	*0.042*	*3*	*0.014*	*1213.81*	*< 0.0001*	*0.022*	*3*	*7.224E-003*	*190.76*	*< 0.0001*	*0.017*	*3*	*5.780E-003*	*198.37*	*< 0.0001*
AB	*5E-005*	*1*	*5.000E-005*	*4.37*	*0.0433*	5.000E-005	*1*	*5.000E-005*	*1.32*	*0.2577*	*1.125E-004*	*1*	*1.125E-004*	*3.86*	*0.0568*
AC	*1.25E-005*	*1*	*1.250E-005*	*1.09*	*0.3025*	5.000E-005	*1*	*5.000E-005*	*1.32*	*0.2577*	*0.000*	*1*	*0.000*	*0.000*	*1.0000*
AD	*3.031E-003*	*3*	*1.010E-003*	*88.32*	*< 0.0001*	*2.037E-003*	*3*	*6.792E-004*	*17.93*	*< 0.0001*	*5.188E-004*	*3*	*1.729E-004*	*5.93*	*0.0020*
BC	*1.250E-005*	*1*	1.250E-005	*1.09*	*0.3025*	5.000E-005	*1*	*5.000E-005*	*1.32*	*0.2577*	*2.000E-004*	*1*	*2.000E-004*	*6.86*	*0.0126*
BD	*3.125E-005*	*3*	*1.042E-005*	*0.91*	*0.4450*	1.813E-004	*3*	*6.042E-005*	*1.6*	*0.2065*	*6.875E-005*	*3*	*2.292E-005*	*0.79*	*0.5089*
CD	*2.375E-004*	*3*	*7.917E-005*	*6.92*	*0.0008*	*5.562E-004*	*3*	*1.854E-004*	*4.9*	*0.0057*	*2.250E-004*	*3*	*7.500E-005*	*2.57*	*0.0682*
A^2	*1.368E-005*	*1*	1.368E-005	*1.20*	*0.2811*	*3.077E-005*	*1*	*3.077E-005*	*0.81*	*0.3731*	*4.720E-004*	*1*	*4.720E-004*	*16.20*	*0.0003*
B^2	*4.137E-004*	*1*	4.137E-004	*36.16*	*< 0.0001*	*5.889E-004*	*1*	*5.889E-004*	*15.55*	*0.0003*	*3.026E-003*	*1*	*3.026E-003*	*103.85*	*< 0.0001*
C^2	*1.368E-005*	*1*	*1.368E-005*	*1.20*	*0.2811*	*1.389E-004*	*1*	*1.389E-004*	*3.67*	*0.0630*	*1.797E-004*	*1*	*1.797E-004*	*6.17*	*0.0175*
Residual	*4.347E-004*	*38*	1.144E-005			*1.439E-003*	*38*	*3.787E-005*			*1.107E-003*	*38*	*2.914E-005*		
Std. Dev	*3.382E-003*					*6.154E-003*					*5.398E-003*				
PRESS	*1.050E-003*					*3.858E-003*					*2.736E-003*				
R-square	*0.9988*					*0.9969*					*0.9978*				
Adj- R-square	*0.9982*					*0.9952*					*0.9966*				
Pred- R-square	*0.9972*					*0.9917*					*0.9946*				

A: Interior thickness; B: Concrete Thickness; C: Exterior thickness; D: Type of Mortar.

- OPBCM-NM:

$$\varnothing = \left[-0.06219 + \left(0.04^{*}d_{m,in}\right) + \left(0.028471^{*}d_{c}\right) + \left(0.02^{*}d_{m,ext}\right) - \left((1.90698E-005)^{*}d_{c}^{2}\right)\right] \quad (21)$$

- OPBCM-OPBCM:

$$\varnothing = \left[-0.012969 + \left(0.04125^{*}d_{m,in}\right) + \left(0.028471^{*}d_{c}\right) + \left(0.03125^{*}d_{m,ext}\right) - \left((1.90698E-005)^{*}d_{c}^{2}\right)\right] \quad (22)$$

➢ For OPBCC1:

- NM-NM:

$$\varnothing = \left[-0.50208 + \left(0.026250^{*}d_{m,in}\right) + \left(0.033375^{*}d_{c}\right) + \left(0.03125^{*}d_{m,ext}\right)\right] \quad (23)$$

- NM-OPBCM:

$$\varnothing = \left[-0.46375 + \left(0.0225^{*}d_{m,in}\right) + \left(0.033375^{*}d_{c}\right) + \left(0.04^{*}d_{m,ext}\right)\right] \quad (24)$$

- OPBCM-NM:

$$\varnothing = \left[-0.48708 + \left(0.041250^{*}d_{m,in}\right) + \left(0.033375^{*}d_{c}\right) + \left(0.03125^{*}d_{m,ext}\right)\right] \quad (25)$$

- OPBCM-OPBCM:

$$\varnothing = \left[-0.45292 + \left(0.0425^{*}d_{m,in}\right) + \left(0.033375^{*}d_{c}\right) + \left(0.0375^{*}d_{m,ext}\right)\right] \quad (26)$$

➢ For OPBCC2:

- NM-NM:

$$\varnothing = \left[-0.57292 + \left(0.035^{*}d_{m,in}\right) + \left(0.041875^{*}d_{c}\right) + \left(0.03125^{*}d_{m,ext}\right) - \left((7.5E-005)^{*}d_{m,in}{}^{*}d_{c}\right)\right] \quad (27)$$

- NM-OPBCM:

$$\varnothing = \left[-0.62042 + \left(0.03625^{*}d_{m,in}\right) + \left(0.0421255^{*}d_{c}\right) + \left(0.04^{*}d_{m,ext}\right) - \left((7.5E-005)^{*}d_{m,in}{}^{*}d_{c}\right)\right] \quad (28)$$

- OPBCM-NM:

$$\varnothing = \left[-0.65042 + \left(0.05125^{*}d_{m,in}\right) + \left(0.0426255^{*}d_{c}\right) + \left(0.03^{*}d_{m,ext}\right) - \left((7.5E-005)^{*}d_{m,in}{}^{*}d_{c}\right)\right] \quad (29)$$

- OPBCM-OPBCM:

$$\varnothing = \left[-0.46875 + \left(0.05125^{*}d_{m,in}\right) + \left(0.0411255^{*}d_{c}\right) + \left(0.04^{*}d_{m,ext}\right) - \left((7.5E-005)^{*}d_{m,in}{}^{*}d_{c}\right)\right] \quad (30)$$

5.3.2. Analysis of variance (ANOVA) for decrement factor (f)

Table 8 shows that the significant model terms are A, B, C, D, AB, AD, CD, and B^2 for regular concrete. In the case of OPBCC1, the significant model parameters are A, B, C, D, AD, CD, and B^2. Regarding OPBCC2, the multiple parameters are A, B, C, D, AD, BC, A^2, B^2, and C^2. Like the time lag, the concrete thickness significantly impacts the decrement factor of a wall system. The agreement between R-squared and adjusted R-squared confirmed the accuracy of the proposed model for predicting the decrement factor. Fig. 4 shows the actual values versus the predicted values.

The following equations (equations (31)–(42)) can be applied to predict the decrement factor of wall systems.

➢ For NC:

- NM-NM:

$$f = \left[1.20627 - \left((4.0E-003)^{*}d_{m,in}\right) - \left((4.09331E-003)^{*}d_{c}\right) - \left((2.25E-003)^{*}d_{m,ext}\right) + \left((1.0E-005)^{*}d_{m,in}{}^{*}d_{c}\right) + \left((4.186E-006)^{*}d_{c}^{2}\right)\right] \quad (31)$$

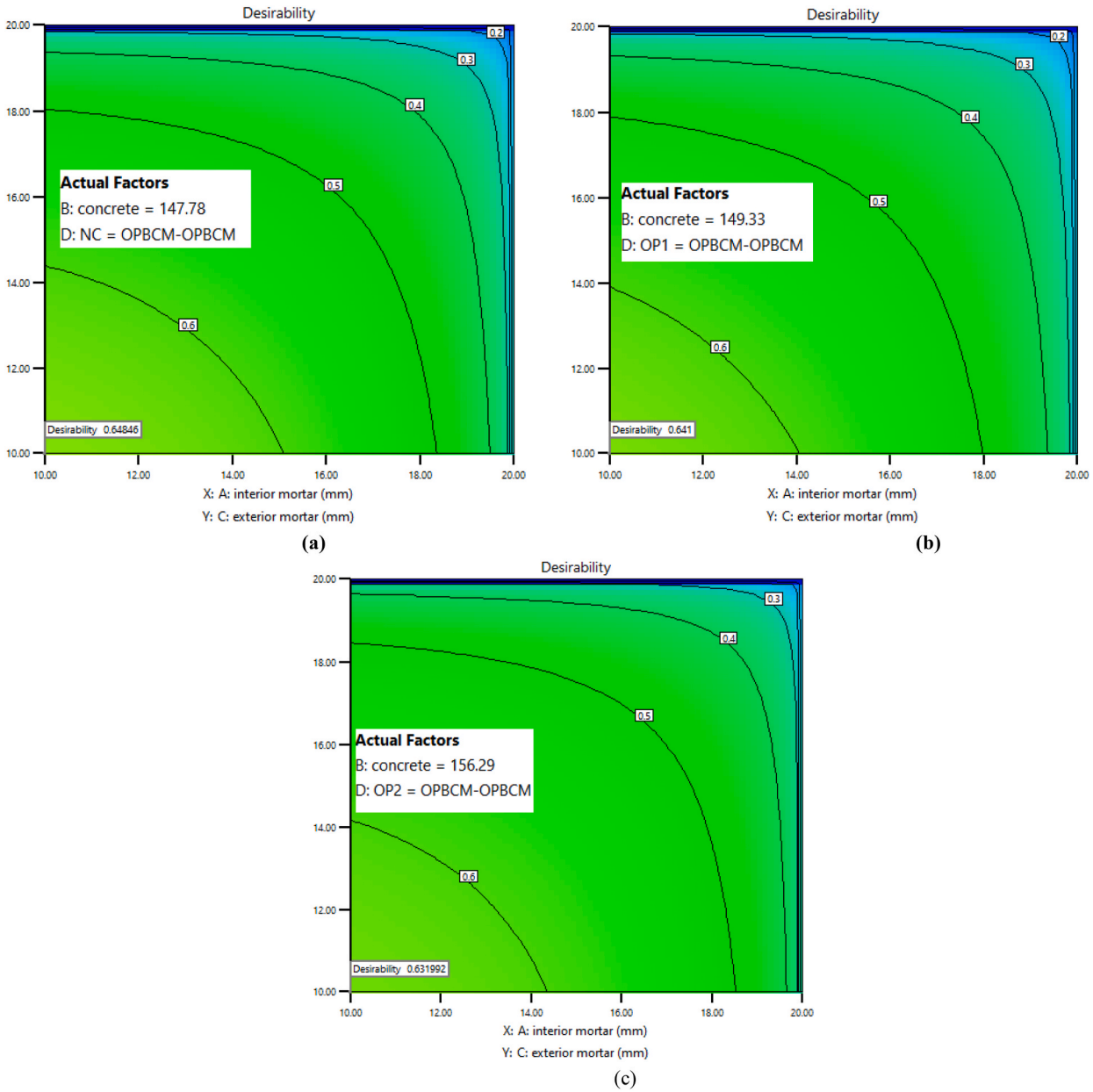

Fig. 5. Optimization for a) NC, b) OPBCC1, c) OPBCC2.

- NM-OPBCM:

$$f=\left[1.21194-\left((4.125E-003)*d_{m,in}\right)-((4.09331E-003)*d_c)-\left((3.125E-003)*d_{m,ext}\right)+((1.0E-005)*d_{m,in}*d_c)\right.$$
$$\left.+\left((4.186E-006)*d_c^2\right)\right] \quad (32)$$

- OPBCM-NM:

$$f=\left[1.20060-\left((6.750E-003)*d_{m,in}\right)-((4.09331E-003)*d_c)-\left((2.50E-003)*d_{m,ext}\right)+\left((1.0E-005)*d_{m,in}*d_c\right)+\left((4.186E-006)*d_c^2\right)\right] \quad (33)$$

- OPBCM-OPBCM:

$$f = \left[1.20052 - \left((6.8750E-003)^{*}d_{m,in}\right) - \left((4.09331E-003)^{*}d_c\right) - \left((3.125E-003)^{*}d_{m,ext}\right) + \left((1.0E-005)^{*}d_{m,in}{}^{*}d_c\right) + \left((4.186E-006)^{*}d_c^2\right)\right] \quad (34)$$

➢ For OPBCC1:

- NM-NM:

$$f = \left[1.21952 - \left((1.75E-003)^{*}d_{m,in}\right) - \left((4.44331E-003)^{*}d_c\right) - \left((2.25E-003)^{*}d_{m,ext}\right) + \left((4.186E-006)^{*}d_c^2\right)\right] \quad (35)$$

- NM-OPBCM:

$$f = \left[1.22735 - \left((1.75E-003)^{*}d_{m,in}\right) - \left((4.44331E-003)^{*}d_c\right) - \left((3.75E-003)^{*}d_{m,ext}\right) + \left((4.186E-006)^{*}d_c^2\right)\right] \quad (36)$$

- OPBCM-NM:

$$f = \left[1.23227 - \left((4.125E-003)^{*}d_{m,in}\right) - \left((4.44331E-003)^{*}d_c\right) - \left((3.125E-003)^{*}d_{m,ext}\right) + \left((4.186E-006)^{*}d_c^2\right)\right] \quad (37)$$

- OPBCM-OPBCM

$$f = \left[1.22269 - \left((3.875E-003)^{*}d_{m,in}\right) - \left((4.44331E-003)^{*}d_c\right) - \left((3.625E-003)^{*}d_{m,ext}\right) + \left((4.186E-006)^{*}d_c^2\right)\right] \quad (38)$$

➢ For OPBCC2:

- NM-NM:

$$f = \left[1.45189 - \left((6.16667E-003)^{*}d_{m,in}\right) - \left((7.65417E-003)^{*}d_c\right) - \left((8.29167E-003)^{*}d_{m,ext}\right) + \left((2.0E-005)^{*}d_c{}^{*}d_{m,ext}\right) + \left((1.30556E-004)^{*}d_{m,in}^2\right) + \left((1.32222E-005)^{*}d_c^2\right) + \left((8.05556E-005)^{*}d_{m,ext}^2\right)\right] \quad (39)$$

- NM-OPBCM:

$$f = \left[1.43656 - \left((6.16667E-003)^{*}d_{m,in}\right) - \left((7.65417E-003)^{*}d_c\right) - \left((8.29167E-003)^{*}d_{m,ext}\right) + \left((2.0E-005)^{*}d_c{}^{*}d_{m,ext}\right) + \left((1.30556E-004)^{*}d_{m,in}^2\right) + \left((1.32222E-005)^{*}d_c^2\right) + \left((8.05556E-005)^{*}d_{m,ext}^2\right)\right] \quad (40)$$

- OPBCM-NM:

$$f = \left[1.43931 - \left((7.41667E-003)^{*}d_{m,in}\right) - \left((7.65417E-003)^{*}d_c\right) - \left((8.29167E-003)^{*}d_{m,ext}\right) + \left((2.0E-005)^{*}d_c{}^{*}d_{m,ext}\right) + \left((1.30556E-004)^{*}d_{m,in}^2\right) + \left((1.32222E-005)^{*}d_c^2\right) + \left((8.05556E-005)^{*}d_{m,ext}^2\right)\right] \quad (41)$$

- OPBCM-OPBCM:

$$f = \left[1.42156 - \left((7.1667E-003)^{*}d_{m,in}\right) - \left((7.65417E-003)^{*}d_c\right) - \left((8.29167E-003)^{*}d_{m,ext}\right) + \left((2.0E-005)^{*}d_c{}^{*}d_{m,ext}\right) + \left((1.30556E-004)^{*}d_{m,in}^2\right) + \left((1.32222E-005)^{*}d_c^2\right) + \left((8.05556E-005)^{*}d_{m,ext}^2\right)\right] \quad (42)$$

5.3.3. Sensitivity analysis

The sensitivity analysis was carried out by RSM output to find the effect of each parameter on the time lag and decrement factor of a wall system. The contribution of each element is calculated by considering the rate of the sum of the square for each parameter and the total sum of the square (Tables 7 and 8). Also, all parameters should be contained the same degree of freedom for analyzing the sensitivity [33].

It should be considered that the sensitivity of the wall system has been evaluated in minimum, medium, and maximum thickness of concrete when the interior and exterior thickness of cement plaster are in the ranges of 10–20 mm. The results indicated the time lag of a wall system (containing 10 mm plaster at both sides) increased around 30.6% when the NC thicknesses changed from 125 mm to 175 mm. However, the time lag increment was approximately 39.3% and 38.5% for wall systems containing OPBCC1 and OPBCC2, respectively. Also, the decrement factor reduction for a wall system (10 mm plaster at both sides) comprising NC, OPBCC1, and

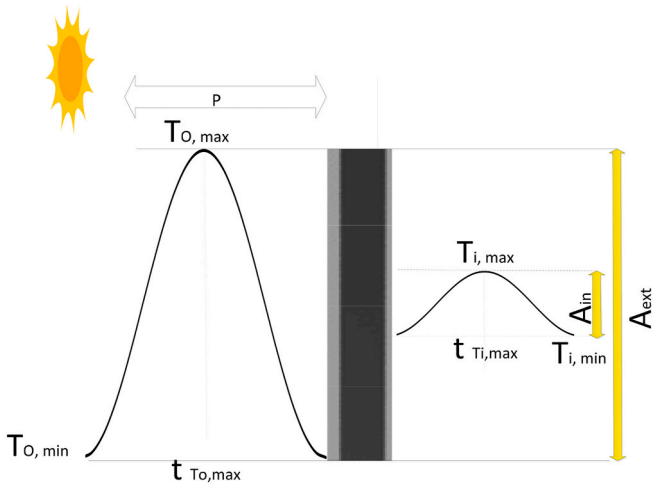

Fig. 6. Schematic of heatwave transferring.

OPBCC2 was respectively around 19.1%, 23.5%, and 30%; the thicknesses changed from 125 mm to 175 mm.

The sensitivity analysis specified that the concrete thickness significantly impacts a wall system's time lag and decrement factor. Thus, the optimization results depend on the concrete thickness over other parameters. The criteria for optimization were minimizing the wall system (minimum concrete thickness and interior and exterior plaster thickness), minimizing the decrement factor, and maximizing time lag. The optimum situations with a desirability of around 0.6 are shown in Fig. 5.

5.4. Indoor air temperature

A typical wall system constructed with 150 mm of concrete and plastered with 12.5 mm of cement mortar on both sides was assumed to evaluate the effect of OPBC on the indoor temperature in Kuala Lumpur. A heatwave schematic transferring through a wall is shown in Fig. 6. The developed statistical equations were used to calculate a wall system's time lag and decrement factor. Then, based on the decrement factor and time lag, the indoor air temperature is calculated using the following equation:

$$T(t) = T_{av} + |T| Cos\ (\omega t + \varphi) \tag{42}$$

The achieved indoor temperatures in different hours are shown in Fig. 7. The results indicated that OPBC mortar and concrete significantly decreased the indoor peak temperature by around 0.5 °C. Not surprisingly, the OPBC wall system is predictable to postpone the peak temperature dramatically. This application can help construct energy-efficient office buildings since office buildings are usually operational between 9 a.m. and 6 p.m. in Malaysia. Besides, the results implied indoor air temperature of the OPBC wall is around 3% and 8% lower than the typical wall at 9 a.m. and 12 p.m., respectively. An OPBC wall system can decrease the indoor air temperature by around 14% compared to the outdoor air temperature at the peak hour. It should be noted that the typical wall system reduction is just approximately 5.5%.

6. Conclusion

This study evaluated the time lag (φ) and decrement factor (f) of cement mortar and concrete containing oil palm boiler clinker (OPBC) as fine aggregate and coarse aggregate through EN ISO 13768. The results of this study can be concluded as follow:

The thermal conductivity of oil palm boiler clinker mortar (OPBCM) compared to ordinary mortar (NM) decreased by around 14% and 72%, respectively. The density reduction for concrete containing OPBC as coarse aggregate (OPBCC1) and concrete containing OPBC as fine and coarse aggregate (OPBCC2) compared to the NC is around 18.7% and 21%, respectively. Also, the thermal conductivity reduction of OPBCC1 and OPBCC2 compared to the NC was 64% and 77%, respectively. Furthermore, the heat capacity of OPBCC1 and OPBCC2 was around 1% and 23% more than NC.

The φ of NM and OPBCM is between 0.09 to 0.49 h and 0.1–0.62 h, respectively. Also, the φ of NC, OPBCC1 and OPBCC2 are in the range of 2.49–4.92 h, 2.85–6.25 h, and 3.65–7.80 h, respectively. It should be noted that the cement mortar was in the range of 5–25 mm, and the concrete was in the range of 100–200 mm.

In summary, the results of this study indicated that the OPBC mortar and concrete could provide thermal comfort and reduce energy consumption when applied in load-bearing or non-load-bearing wall systems. For instance, the indoor air temperature decreased by around 14% compared to the outdoor air temperature at the peak hour using the OPBC wall system. Therefore, the results of this study can be a reasonable practice and reference for applying proper materials for wall systems to reduce energy consumption in the building sector of Malaysia and move toward energy-efficient buildings.

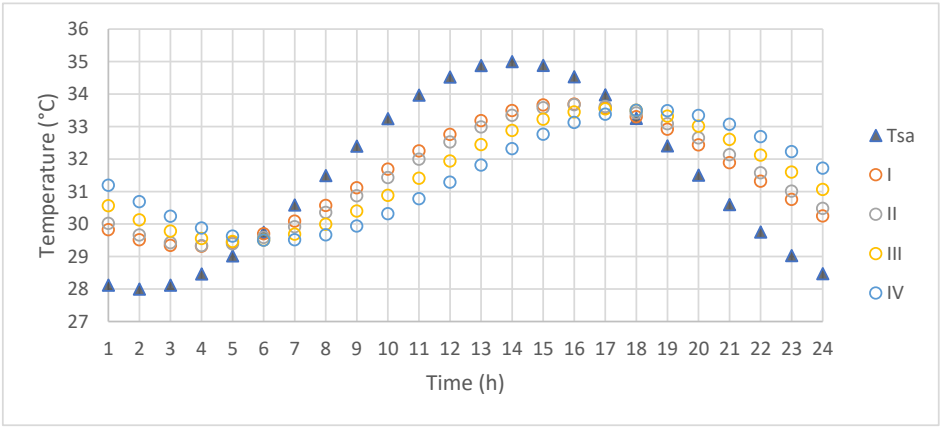

(a)

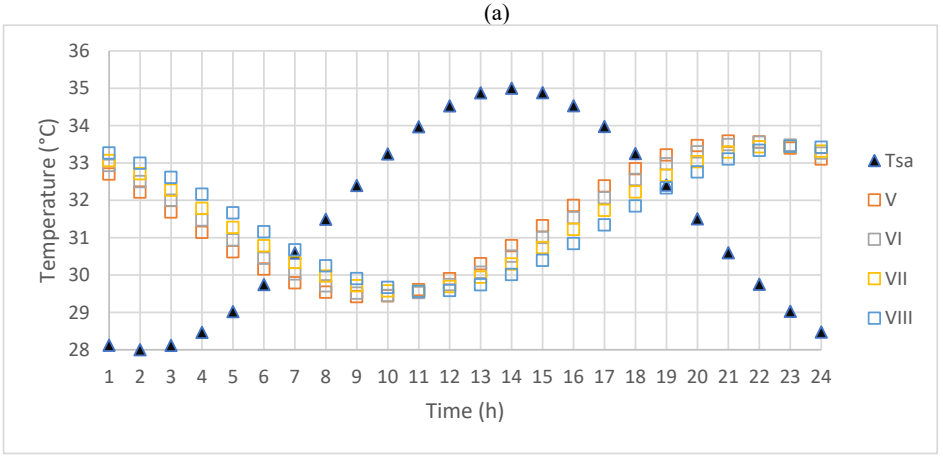

(b)

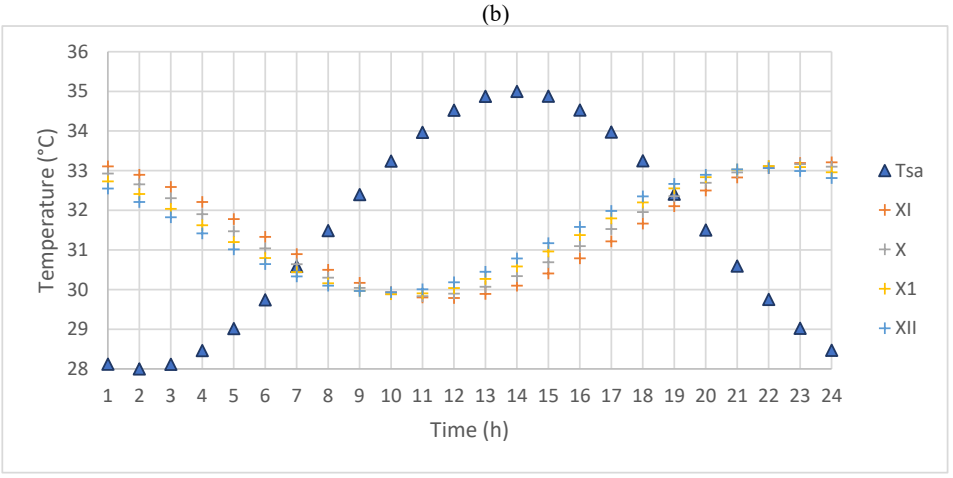

(c)

Fig. 7. Indoor air temperature for a) NC, b) OPBCC1, and c) OPBCC2.

Author statement

Iman Asadi: Conceptualization, Methodology, Software, Formal analysis, Investigation, Writing - Original Draft. Mohammad Hashemi: Methodology, Validation, Investigation, Writing - Original Draft. Behran sajadi: Writing - Review & Editing, Funding acquisition. Norhayati Binti Mahyuddin: Resources, Supervision. Mohammad Hajmohammadian Baghban: Review & Editing. Masoud Esfandiari: Review & Editing, Formal analysis. Mehdi Maghfouri: Writing - Review & Editing, Data Curation. Kezhen Yan: Writing - Review & Editing.

Declaration of competing interest

The authors declare that they have no known competing financial interests or personal relationships that could have appeared to influence the work reported in this paper.

Data availability

No data was used for the research described in the article.

Appendix A. Supplementary data

Supplementary data to this article can be found online at https://doi.org/10.1016/j.csite.2022.102609.

References

[1] P. Shafigh, et al., Thermal properties of cement mortar with different mix proportions, Mater. Construcción 70 (339) (2020) 224.
[2] J. de Brito, R. Kurda, The past and future of sustainable concrete: a critical review and new strategies on cement-based materials, J. Clean. Prod. 281 (2021), 123558.
[3] P. Shafigh, I. Asadi, N.B. Mahyuddin, Concrete as a thermal mass material for building applications-A review, J. Build. Eng. 19 (2018) 14–25.
[4] K.-H. Kim, et al., An experimental study on thermal conductivity of concrete, Cement Concr. Res. 33 (3) (2003) 363–371.
[5] J. Chan, Thermal properties of concrete with different Swedish aggregate materials. Rapport TVBM (5000-serie), 2014.
[6] P. Shafigh, et al., Structural lightweight aggregate concrete using two types of waste from the palm oil industry as aggregate, J. Clean. Prod. 80 (2014) 187–196.
[7] K. Muthusamy, N. Zulkepli, F. Mat Yahaya, Exploratory study of oil palm shell as partial sand replacement in concrete, Res. J. Appl. Sci. Eng. Technol. 5 (7) (2013) 2372–2375.
[8] H. Mahmud, M.Z. Jumaat, U. Alengaram, Influence of sand/cement ratio on mechanical properties of palm kernel shell concrete, J. Appl. Sci. 9 (9) (2009) 1764–1769.
[9] M. Aslam, et al., Manufacturing of high-strength lightweight aggregate concrete using blended coarse lightweight aggregates, J. Build. Eng. 13 (2017) 53–62.
[10] P. Shafigh, et al., A comparison study of the fresh and hardened properties of normal weight and lightweight aggregate concretes, J. Build. Eng. 15 (2018) 252–260.
[11] M. Aslam, et al., Benefits of using blended waste coarse lightweight aggregates in structural lightweight aggregate concrete, J. Clean. Prod. 119 (2016) 108–117.
[12] H. Hartono, L.J. Chai, B. Lee, Lightweight concrete using oil palm boiler clinker (OPBC)–A review, in: MATEC Web of Conferences, EDP Sciences, 2016.
[13] I. Asadi, et al., Thermophysical properties of sustainable cement mortar containing oil palm boiler clinker (OPBC) as a fine aggregate, Construct. Build. Mater. (2020), 121091.
[14] Soret, G., et al., Thermal inertia as an integrative parameter for building performance. J. Build. Eng.. 33: p. 101623.
[15] H. Asan, Y. Sancaktar, Effects of wall's thermophysical properties on time lag and decrement factor, Energy Build. 28 (2) (1998) 159–166.
[16] H. Asan, Numerical computation of time lags and decrement factors for different building materials, Build. Environ. 41 (5) (2006) 615–620.
[17] R. Duffin, G. Knowles, A passive wall design to minimize building temperature swings, Sol. Energy 33 (3–4) (1984) 337–342.
[18] A.S.f. Testing, M.C.C.-o. Cement, Standard Test Method for Compressive Strength of Hydraulic Cement Mortars (Using 2-in. Or [50-mm] Cube Specimens), ASTM International, 2013.
[19] A. Standard, Standard Test Method for Compressive Strength of Cylindrical Concrete Specimens, ASTM C39, 2010.
[20] S.F. Larsen, C. Filippín, G. Lesino, Thermal behavior of building walls in summer: comparison of available analytical methods and experimental results for a case study, in: Building Simulation, Springer, 2009.
[21] ISO, E., 13786, Thermal Performance of Building Components–Dynamic Thermal Characteristics–Calculation Methods, European Committee for Standardization, 1999.
[22] ISO, E., 6946, Building Components and Building Elements–Thermal Resistance and Thermal Transmittance–Calculation Method, V., Berlin, 2007 (ISO 6946: 2007).
[23] W.d. Koppen, Das geographische system der klimat, Handbuch der klimatologie, 1936, p. 46.
[24] R. Ahmmad, et al., Performance evaluation of palm oil clinker as coarse aggregate in high strength lightweight concrete, J. Clean. Prod. 112 (2016) 566–574.
[25] B.S. Mohammed, et al., Shear strength of palm oil clinker concrete beams, Mater. Des. 46 (2013) 270–276.
[26] B.S. Mohammed, W. Foo, M. Abdullahi, Flexural strength of palm oil clinker concrete beams, Mater. Des. 53 (2014) 325–331.
[27] P. Darvish, et al., Performance evaluation of palm oil clinker sand as replacement for conventional sand in geopolymer mortar, Construct. Build. Mater. 258 (2020), 120352.
[28] P. Darvish, et al., Volume based design approach for sustainable palm oil clinker as whole replacement for conventional sand in mortar, J. Build. Eng. 32 (2020), 101660.
[29] P. Darvish, et al., Enunciation of size effect of sustainable palm oil clinker sand on the characteristics of cement and geopolymer mortars, J. Build. Eng. 44 (2021), 103335.
[30] M. Aslam, P. Shafigh, M.Z. Jumaat, Oil-palm by-products as lightweight aggregate in concrete mixture: a review, J. Clean. Prod. 126 (2016) 56–73.
[31] J. Kanadasan, H.A. Razak, Fresh properties of self-compacting concrete incorporating palm oil clinker, in: InCIEC 2013, Springer, 2014, pp. 249–259.
[32] S. Iranmanesh, et al., Evaluation of viscosity and thermal conductivity of graphene nanoplatelets nanofluids through a combined experimental–statistical approach using respond surface methodology method, Int. Commun. Heat Mass Tran. 79 (2016) 74–80.
[33] J. Liu, et al., A multi-parameter optimization model for the evaluation of shale gas recovery enhancement, Energies 11 (3) (2018) 654.